Measurement of the Pressure Dependence of Viscosity of Polymer Melts Using a Back Pressure-Regulated Capillary Rheometer

Johanna Aho, Seppo Syrjälä

Laboratory of Plastics and Elastomer Technology, Tampere University of Technology, Tampere 33101, Finland

Received 17 March 2009; accepted 12 November 2009
DOI 10.1002/app.31754
Published online 26 March 2010 in Wiley InterScience (www.interscience.wiley.com).

ABSTRACT: The effect of pressure on the melt viscosity was experimentally investigated for five polymers: polycarbonate (PC), acrylonitrile-butadiene-styrene (ABS), polystyrene (PS), polypropylene (PP), and low-density polyethylene (LDPE). Measurements were carried out using capillary rheometer modified to allow regulation of back pressure. To enable correction for the entrance pressure drop, two round-hole dies were used: a 1-mm diameter die of length 10 mm and an orifice die of the same diameter. For determining the pressure coefficient from the experimental viscosity data, time-pressure superposition was applied to generate a master curve to which the Carreau-Yasuda model was fitted. The resulting pressure coefficients revealed that for the polymers studied the order of the degree of the pressure dependence is as follows: PS > ABS > PC > PP > LDPE. © 2010 Wiley Periodicals, Inc. J Appl Polym Sci 117: 1076–1084, 2010

Key words: viscosity; rheology; thermoplastics; injection molding

INTRODUCTION

In recent years, the importance of the pressure dependence of the viscosity of polymer melts has been increasingly recognized. Especially in the injection molding process the polymer melt is frequently subjected to pressures in excess of 100 MPa, which is by far sufficient to markedly increase the melt viscosity. It is clear that the effect of pressure on the viscosity should also be taken into account in the computer simulation of injection molding. This is particularly the case when simulation is applied to thin-wall injection molding, as demonstrated by a recent study utilizing the dimensional analysis approach.[1] Nevertheless, the data available for the pressure dependence of the viscosity of various polymers are still quite scarce, apparently owing to inherent difficulties involved in the high-pressure rheometry.

Basically two types of rheometers exist; those based on drag flow, and those based on pressure-driven flow. For examining the pressure dependence of polymer viscosity, the rheometers of the latter type have been much more commonly used. In the earliest work on the subject, Maxwell and Jung[2] used a modified capillary rheometer consisting of two barrels and two independently controlled pistons, which enabled the melt in the capillary to be pressurized from both sides. Later on, an essentially similar design has been employed by a number of researchers.[3–6] The apparatus of this type, but equipped with a slit die with three pressure transducers mounted along the length of the die, has also been successfully employed.[7] Even though the double-piston rheometers appear to provide a plausible means of determining the pressure dependent viscosity, their use has been rather infrequent. Obvious reasons are the complexities and the operating and maintenance difficulties associated with such instruments.

The simplest and most accessible way of providing information on the pressure dependence of viscosity is undoubtedly through consideration of the nonlinear pressure profile along the capillary[8–11] or slit[12] when the polymer melt flows from a high pressure to atmospheric pressure. These kinds of experiments can be conducted with a standard capillary rheometer. When using round-hole capillary dies, the nonlinearity has to be extracted from the Bagley plots, whereas slit dies allow a direct deduction of the pressure profile, if at least three pressure transducers are mounted on the die wall. The approach based on the nonlinear pressure profile, however, suffers from a poor sensitivity and is useful only for materials which exhibit a relatively large effect of pressure on viscosity. Moreover, the temperature and slip effects may also contribute to the

Correspondence to: J. Aho (johanna.aho@tut.fi).
Contract grant sponsors: Academy of Finland, Graduate School of Processing of Polymers and Polymer-based Multimaterials.

nonlinearity of the pressure profile and it is difficult to separate them from the pressure effects. In the case of the capillary die, when only the reservoir pressure can be measured, a further complication arises from the fact that the entrance pressure drop also depends on the pressure.

The vast majority of recent studies on high-pressure viscosity measurements of polymer melts have used a capillary rheometer, in which a specially constructed assembly with an adjustable valve for regulating the back pressure is attached against the outflow end of the die. This type of arrangement was apparently first used with a slit die,[12] and subsequently with a capillary die by several researchers.[13–20] The main appeal of this approach is that only relatively minor modifications are required to standard capillary rheometers. Yet, all capillary-type instruments also have inherent drawbacks; most notably, the nonuniformity of the pressure and shear rate fields in the test section, and the excess pressure drop associated with the contraction flow at the die entrance. Consequently, corrections to the data are needed to derive the true wall shear stress (Bagley-correction) and the true wall shear rate (Rabinowitsch-correction). The varying pressure naturally complicates the data handling process when just the effect of pressure is to be explored. Despite the deficiencies involved, a back pressure-regulated capillary rheometer offers a reasonable compromise between complexity and accuracy, as noted in a study comparing different measurement techniques for evaluating the pressure dependence of the viscosity.[16]

Drag flow rheometers, which are typically some sort of rotational rheometers, generally have a major advantage over the pressure-driven rheometers in that the pressure and shear rate are uniform throughout the sample, which makes the procedures for data analysis relatively straightforward. Unfortunately, these types of instruments are not easily adaptable to measurements at elevated pressures. For example, the sealing of the rotating parts becomes extremely difficult under high pressure. Consequently, the drag flow rheometers have been rarely used for quantifying the pressure dependence of the viscosity of polymer melts. Nonetheless, there are a few early studies in which the pressurized versions of concentric cylinder rheometers were used.[21–23] With this configuration, however, sample loading and cleaning of the measuring system are laborious and time-consuming. A notable more recent contribution is by Koran and Dealy,[24] who developed a pressurized version of a sliding plate rheometer. This apparatus is clearly an attractive candidate for high-pressure rheometry; pressures up to 70 MPa and shear rates up to 500 s^{-1} are reachable, which is much more than with usual drag flow rheometers. The wider use of the sliding plate rheometer is, however, inhibited by the fact that it is not commercially available.

The pressure dependence of viscosity varies from one polymer to another and is largely determined by the molecular structure. The differences between polymers are often explained by the concept of free volume (the volume unoccupied by polymer molecules) and the idea that the mobility of molecular chains is primarily controlled by the free volume.[25] Relations between free volume and pressure dependence of viscosity have originally been investigated by Utracki,[26] and after that for example by Utracki and Sedlacek.[27] Estimations of pressure dependence of viscosity can be made using the information achieved from pressure–volume–temperature (PVT) measurements.[28,29] Obviously, free volume decreases with increasing pressure just as it does with decreasing temperature. Molecular structures having stiff backbone with aromatic groups or double bond, or bulky pendant groups, necessarily possess more free volume and are thus more susceptible to the volumetric changes with pressure (and temperature). In accordance with this, for example, the values of pressure coefficients reported for polystyrene ($\beta \approx 30$ GPa^{-1}) are consistently higher than those reported for polyethylenes ($\beta < 20$ GPa^{-1}).[15,18]

In this study, a capillary rheometer equipped with a downstream pressure chamber was used to evaluate the pressure dependence of viscosity for five polymers: polycarbonate, acrylonitrile-butadiene-styrene, polystyrene, polypropylene, and low-density polyethylene. A round-hole die, having a length of 10 mm and diameter of 1 mm, and an orifice die of the same diameter were used in the experiments, with the latter one giving directly the entrance pressure drop. To obtain the pressure coefficients, experimental viscosity data were reduced to master curves by means of time-pressure superposition and the Carreau-Yasuda model was fitted to the shifted data.

MATERIALS AND METHODS

Materials

The materials chosen for the study were polycarbonate (PC) Lexan HF1110R supplied by GE Plastics, acrylonitrile-butadiene-styrene (ABS) Terluran GP-22 and polystyrene (PS) Polystyrol 143E by BASF, and polypropylene (PP) Moplen EP340K and low-density polyethylene (LDPE) Lupolen 1840H by Basell. The structural formula for each material is presented in Figure 1. Before measurements, PC and ABS were dried in a desiccator according to the suppliers' recommendations; the first one for 4 h at 120°C and the latter for 4 h at 80°C. No recommendations were

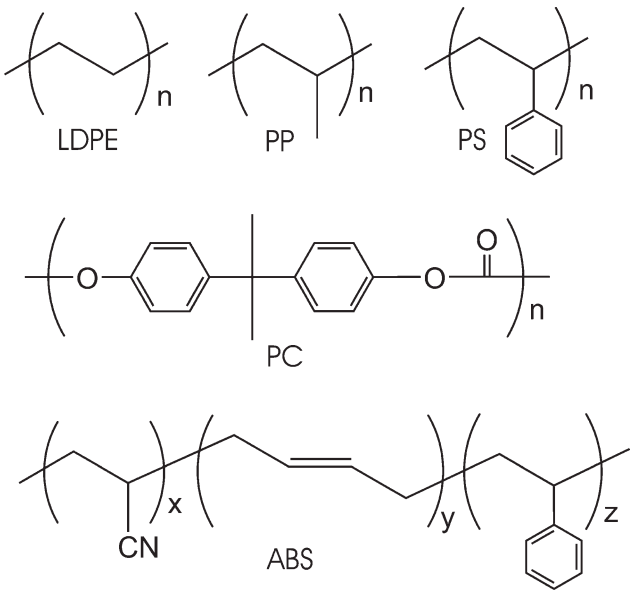

Figure 1 Molecular structural formulas for LDPE, PP, PS, PC, and ABS.

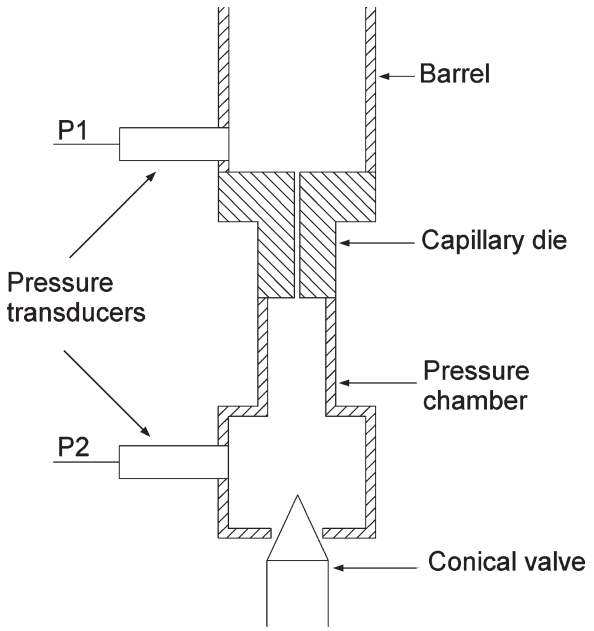

Figure 2 Schematic of the experimental set-up.

given for PS, PP, and LDPE, thus they were not predried. Each material was measured at a single temperature corresponding to a typical processing temperature; temperatures used for PC, ABS, PS, PP, and LDPE were 290, 230, 200, 220, and 200°C, respectively.

Experimental set-up

The high-pressure viscosity measurements were conducted using the Göttfert Rheograph 6000 capillary rheometer modified by the addition of a downstream chamber, also manufactured by Göttfert. The chamber was equipped with an adjustable conical valve to create and vary the back pressure for the melt flow through the capillary die; a schematic of the set-up is shown in Figure 2. Two pressure transducers were installed: first one in the barrel upstream, and the second one in the pressure chamber downstream, of the die. The pressure chamber was maintained at a desired temperature by means of a band heater, which is controlled by a separate thermostat with Pt100 sensor.

During each test run, the piston speed was kept constant, corresponding to a constant apparent shear rate at the die wall. At the beginning of the test, the valve position was chosen such that the back pressure was close to atmospheric. Once the flow had reached a steady state, both transducer readings were recorded simultaneously. The back pressure, and hence the pressure level within the die, was then increased by turning the valve. When stable pressures corresponding to a new valve position were established and recorded, the valve was again turned tighter and this procedure was continued until the barrel emptied or the limit of either pressure transducer was reached. The recommended maximum operating (mean) pressure for the device is 120 MPa. A Teflon ring seal was fitted around the head of the piston to prevent leakage of the melt past the piston so that the piston speed can be used to accurately determine the flow rate through the die.

Tests were performed with two round-hole dies having the same diameter of 1 mm, same entrance angle of 180° and lengths of 10 and 0.2 mm. The latter one is a so-called orifice die (a die with a nominal length of zero; Fig. 3), with which the extra pressure drop at the die entrance can be measured

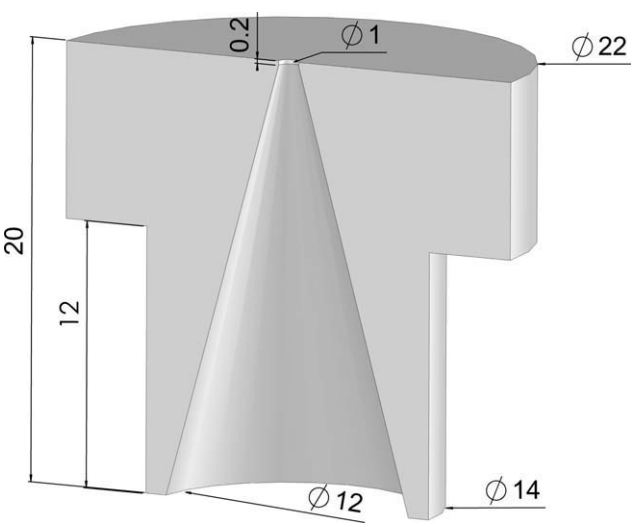

Figure 3 Cross-section of the orifice die used in this study (dimensions in mm).

directly (strictly speaking, some additional pressure drop also occurs at the die exit, but it is typically small compared to the entrance pressure drop). The longer die was chosen to have a relatively small length-to-diameter (L/D) ratio of 10 in order to minimize the distorting effects of viscous heating and pressure dependence of viscosity. Pressure transducers with nominal ranges up to 140 and 100 MPa were employed for upstream and downstream pressure measurement, respectively.

To extend the available shear rate range a rotational rheometer (Anton Paar Physica MCR-301) with a cone-and-plate configuration (diameter 25 mm, angle 2°) was also used to measure the viscosity at low shear rates. These experiments were naturally run at atmospheric pressure.

Analysis of experimental data

Once steady-state conditions have been achieved, a piston moving in the barrel at constant speed generates a constant flow rate, Q, through the die. The apparent shear rate at the die wall can be expressed in terms of the flow rate as

$$\dot{\gamma}_{wa} = \frac{32Q}{\pi D^3} \tag{1}$$

The total pressure drops over the die, that is, Δp_{10} for the 10/1 die and Δp_0 for the orifice die can be written as follows:

$$\Delta p_{10} = p_{u,10} - p_{d,10} \qquad \Delta p_0 = p_{u,0} - p_{d,0} \tag{2}$$

Here, $p_{u,10}$ and $p_{d,10}$, respectively, are the recorded upstream and downstream pressures for the 10/1 die, and $p_{u,0}$ and $p_{d,0}$ the corresponding pressures for the orifice die.

The orifice die used here has a conical outlet expansion section, as depicted in Figure 3. Our previous study comparing the Bagley correction method and the direct measurement with the orifice die showed that this orifice die tends to somewhat overestimate the entrance pressure drop.[30] The increment to the entrance pressure drop arises when the melt adheres to the wall of the outlet section. In normal viscosity measurements (without a pressure chamber), the extent of adherence varies depending on the operating conditions and test material. By contrast, in the measurements with a pressure chamber the outlet section of the orifice die is always full of melt, thus leading to full adherence and maximum overestimation of the entrance pressure drop. In the previous study,[30] utilizing also the numerical flow simulation, we suggested that as an ad hoc correction procedure the entrance pressure drop measured by means of the present orifice die, Δp_0, could be approximated to be 1.5 times the actual entrance pressure drop, Δp_E, when the outlet section of the orifice die is full of melt during the experiment. This procedure is applied here, that is, the entrance pressure drop is taken to be

$$\Delta p_E = \frac{\Delta p_0}{1.5} \tag{3}$$

When measurements with both dies at a given apparent wall shear rate have been carried out, the corrected pressure drop, Δp, corresponding to the fully developed flow in the 10/1 die, can be obtained as

$$\Delta p = \Delta p_{10} - \Delta p_E \tag{4}$$

To rigorously deal with this equation, Δp_{10} and Δp_E should be available at the same upstream pressures. In principle, this could be achieved by suitable valve adjustments, but in practice such conditions turned out to be extremely difficult to realize, because the upstream pressure cannot be directly regulated in the present measuring system. As a consequence, this approach was abandoned and the experiments with both dies were conducted at arbitrary valve settings, and thus at arbitrary upstream pressures. To enable proper data handling, fits to the experimental pressure data of both dies at various apparent wall shear rates were performed using the equations of the form:

$$\begin{aligned} \ln(\Delta p_{10}) &= a_o + a_1 p_{u,10} + a_2 p_{u,10}^2 \\ \ln(\Delta p_E) &= b_o + b_1 p_{u,0} + b_2 p_{u,0}^2 \end{aligned} \tag{5}$$

Here, a_0, a_1, a_2, b_0, b_1, and b_2 are the fitting constants. This type of equations were chosen because the measured data of $\ln(\Delta p_{10})$ versus $p_{u,10}$ and $\ln(\Delta p_E)$ versus $p_{u,0}$ did not strictly fall on straight lines. By applying these fits, Δp_{10} and Δp_E can be extracted at any upstream pressure.

Subsequently, the true shear stress at the die wall can be calculated as

$$\tau_w = \frac{\Delta p}{4L/D} \tag{6}$$

and the apparent viscosity as

$$\eta_a = \frac{\tau_w}{\dot{\gamma}_{wa}} \tag{7}$$

To obtain the true viscosity as a function of true shear rate, a correction for the nonparabolic velocity profile within the die is needed. This is customarily accomplished by means of the Rabinowitsch correction, which requires numerical differentiation of the measured data. A simpler, yet reasonably accurate

alternative, has been proposed by Schümmer and coworkers.[31,32] This procedure is based on estimating the shear rate and viscosity at a radial distance r_s where the apparent shear rate equals the true shear rate. Hence, considering that under fully developed conditions the apparent shear rate, as well as the shear stress, varies linearly with radial position, one obtains

$$\eta(\dot{\gamma} = x^*\dot{\gamma}_{wa}) = \frac{x^*\tau_w}{x^*\dot{\gamma}_{wa}} = \eta_a(\dot{\gamma}_{wa}) \tag{8}$$

where $x^* = r_s/R$ with R being the radius of the die. It appears that x^* varies by only a small amount, so that a representative value of x^* may be chosen for most materials with very little loss in accuracy; the commonly used value $x^* = 0.83$ is adopted for the present study. Note that the Schümmer approximation shifts data only horizontally (to the left) and can be applied to single points.

Determination of pressure coefficient

The results for the pressure dependence of viscosity are usually presented in terms of the pressure coefficient, β. As discussed by Hieber,[33] the pressure coefficient can be defined in different ways: the pressure coefficient for the zero-shear-rate viscosity, β_0, the pressure coefficient at constant shear rate, β', and the pressure coefficient at constant shear stress, β''. These are defined as follows:

$$\beta_o \equiv \left(\frac{\partial \ln \eta_o}{\partial p}\right)_T \qquad \beta' \equiv \left(\frac{\partial \ln \eta}{\partial p}\right)_{\dot{\gamma},T}$$
$$\beta'' \equiv \left(\frac{\partial \ln \eta}{\partial p}\right)_{\tau,T} \tag{9}$$

The first equation is straightforward to use if the experimental zero-shear-rate viscosity data are available at different pressures. Unfortunately, such data rarely exist in practice. The second equation also directly provides the values of pressure coefficients if the measured data were obtained at fixed shear rates, as is usually the case in capillary rheometry. However, the usefulness of the pressure coefficient β' is limited by the fact that it varies with shear rate and is therefore not a real thermodynamic property of the polymer.[16,20] The third equation is equivalent with the first one, that is, $\beta'' = \beta_0$.[33] Its direct use is, however, complicated by the fact that the data from capillary rheometer experiments are normally available at constant shear rates, not at constant shear stresses. In principle, by appropriate fitting procedures, the standard capillary data can be converted in the form that allows the calculation of β'' from the above equation.[20] It is worth noting that in the limits of the zero-shear-rate viscosity region and the power-law region, β' becomes independent of shear rate and can be related to β'' as $\beta'' = \beta'$ and $\beta'' = \beta'/n$, respectively.[15,20,33] An alternative way is to adopt the superposition method, which yields the pressure coefficients similar to β''.[20]

In this work, the last-mentioned approach was invoked: the time-pressure superposition principle was applied to produce a master curve of reduced viscosity η_r ($\equiv \eta/\alpha_p$) versus reduced shear rate $\dot{\gamma}_r(\equiv \alpha_p\dot{\gamma})$ at reference pressure $p_0 = 0.1$ MPa. The pressure shift factor, α_p, was related to the pressure coefficient β by the exponential relation

$$\alpha_p = \exp[\beta(p - p_0)] \tag{10}$$

which is often called the Barus equation (note that, as usual, the vertical shift factor was taken to be unity). In addition, the Carreau-Yasuda viscosity model was fitted to the shifted data points according to

$$\eta_r = \eta_0[1 + (\lambda\dot{\gamma}_r)^a]^{(n-1)/a} \tag{11}$$

where η_0, n, λ, and a are the adjustable parameters. To find the best-fit parameters of eqs. (10) and (11), the method of least squares was used to minimize the overall difference between the shifted experimental data and the Carreau-Yasuda model predictions.

It is worth pointing out that the pressure p in eq. (10) is the mean pressure, p_m. Because mean pressure in the die can not be measured directly, it must be determined in terms of measurable pressure data. Assuming a linear pressure profile in the die, which is clearly justifiable here given the relatively small L/D ratio of the die, the mean pressure can simply be obtained as the arithmetic mean of the pressures at the inlet and outlet of the die. Hence, we can write

$$p_m = \frac{p_{u,10} - \Delta p_E + p_{d,10}}{2} = p_{u,10} - \Delta p_E - \frac{\Delta p}{2} \tag{12}$$

RESULTS AND DISCUSSION

As described earlier, each test run was carried out keeping the piston speed, and hence the apparent wall shear rate, fixed, and gradually increasing the level of back pressure by valve adjustment. For all materials, capillary rheometer experiments were performed at apparent wall shear rates of 50, 100, 200, and 500 s^{-1} (for PC, additionally 1000 s^{-1}). As an example, plots of the measured data of $\ln(\Delta p_{10})$ against $p_{u,10}$ and $\ln(\Delta p_E)$ against $p_{u,0}$ at apparent wall

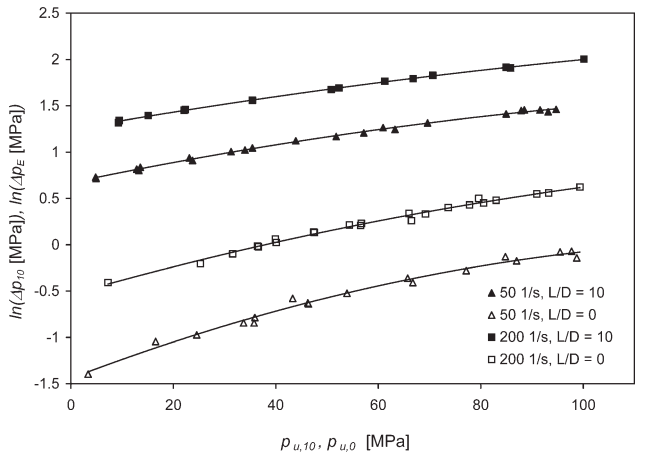

Figure 4 Experimental data of $\ln(\Delta p_{10})$ against $p_{u,10}$ and $\ln(\Delta p_E)$ against $p_{u,0}$ for PP at apparent wall shear rates of 50 and 200 s^{-1}; the lines represent the corresponding fits according to eq. (5).

shear rates of 50 and 200 s^{-1} are provided for PP in Figure 4 together with the corresponding fitted curves based on eq. (5). Similar fits were generated for all polymers at each apparent wall shear rate to facilitate the further handling of the data.

As mentioned earlier, rotational rheometer was used in order to achieve low-shear rate data for enhancing the fitting quality. However, these experiments were excluded in the case of PC, as the zero-shear-rate viscosity was reachable already with the capillary rheometer. On the other hand, for ABS, the zero-shear-rate viscosity could not be attained even with the rotational rheometer: the viscosity of ABS was measured down to a shear rate of 10^{-5} s^{-1} without any indication of leveling off towards a constant value. This kind of behavior is not surprising, since the existence of the yield stress and the consequent disappearance of the zero-shear-rate viscosity with increasing butadiene content has been reported for this polymer.[34] In this case the fitting according to the Carreau-Yasuda model becomes meaningless, because three of the adjustable parameters (η_o, λ, and a) cannot be uniquely determined. Consequently, in the fits for ABS, the Carreau-Yasuda model, eq. (11), was replaced by the power-law expression

TABLE I
Best-Fit Parameters of Equations (10), (11), and (13)

	PC	PS	PP	LDPE	ABS
η_o (Pa s)	215	5300	5190	10,150	–
n (–)	0.200	0.290	0.244	0.360	0.313
a (–)	1.01	0.644	0.537	0.622	–
λ (s)	0.000435	0.200	0.141	0.736	–
K (Pa s^n)	–	–	–	–	20,065
β (GPa^{-1})	26.6	35.5	20.5	17.6	33.7

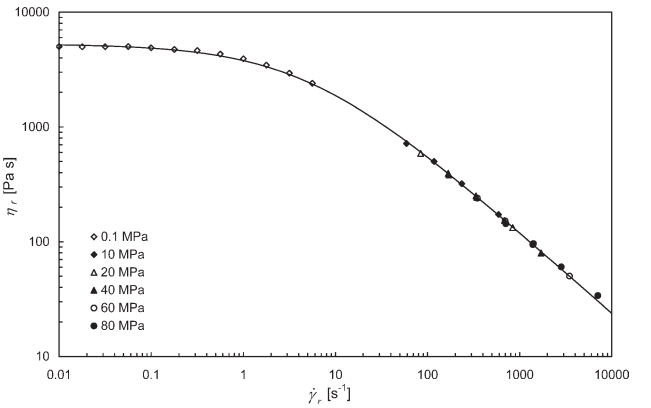

Figure 5 Reduced viscosity (= η/α_p) vs. reduced shear rate (=$\alpha_p\dot{\gamma}$) for PS with eq. (10); the line represents the prediction of the Carreau-Yasuda model, eq. (11). The best-fit parameter values are given in Table I.

$$\eta_r = K\dot{\gamma}_r^{n-1} \tag{13}$$

where K and n are the adjustable parameters.

The values of the adjustable parameters obtained by means of least-squares fits of the viscosity data are presented in Table I for different polymers. The resulting shifted experimental data points as well as the predictions of the Carreau-Yasuda model are shown in Figures 5–9. In general, data from different pressures superpose pretty well onto each other to form a master plot. Likewise, the Carreau-Yasuda model with given parameter values appears to nicely describe the shifted viscosity data of PS, PC, PP, and LDPE, including the low shear rate data from the rotational rheometer. In the case of ABS, however, the data from the rotational and capillary rheometers could not be simultaneously represented by the power-law model. Consequently, only the capillary data were used for fitting and determining the values of the parameters β, n, and K. Even

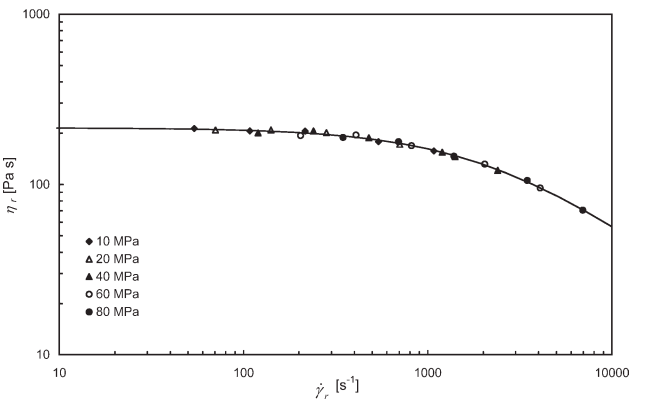

Figure 6 Reduced viscosity (= η/α_p) vs. reduced shear rate (=$\alpha_p\dot{\gamma}$) for PC with eq. (10); the line represents the prediction of the Carreau-Yasuda model, eq. (11). The best-fit parameter values are given in Table I.

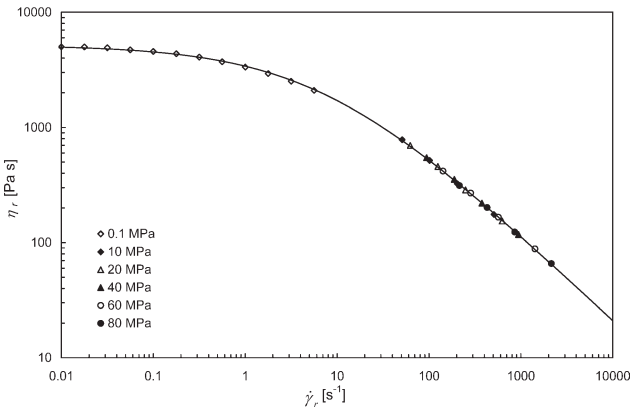

Figure 7 Reduced viscosity (= η/α_p) vs. reduced shear rate (=$\alpha_p\dot{\gamma}$) for PP with eq. (10); the line represents the prediction of the Carreau-Yasuda model, eq. (11). The best-fit parameter values are given in Table I.

though not included in the fits for ABS, selected data points from the rotational rheometer tests are also shown in Figure 9.

The pressure coefficient values are compared in Table II with some previously published data.[7,15,18] It is worth noting that in all of these investigations, measurements were made at several temperatures. According to Hieber,[33] β increases with decreasing T, which apparently means that an accurate simultaneous fit to the data from different temperatures cannot be achieved with a single value of β. In two of these studies,[15,18] the values of β were determined separately for each measurement temperature; the results provided in Table II are taken from temperatures similar or nearest to the present ones. In a study of Kadijk and van den Brule,[7] a more general model was fitted simultaneously to the entire set of data. The authors, however, provided an expression [eq. (10) in their article] which can be used to back

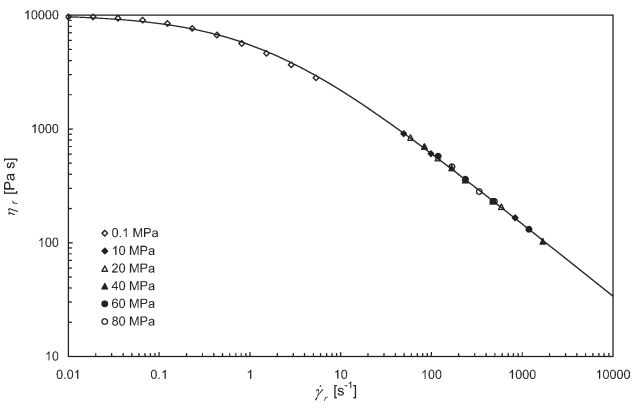

Figure 8 Reduced viscosity (= η/α_p) vs. reduced shear rate (=$\alpha_p\dot{\gamma}$) for LDPE with eq. (10); the line represents the prediction of the Carreau-Yasuda model, eq. (11). The best-fit parameter values are given in Table I.

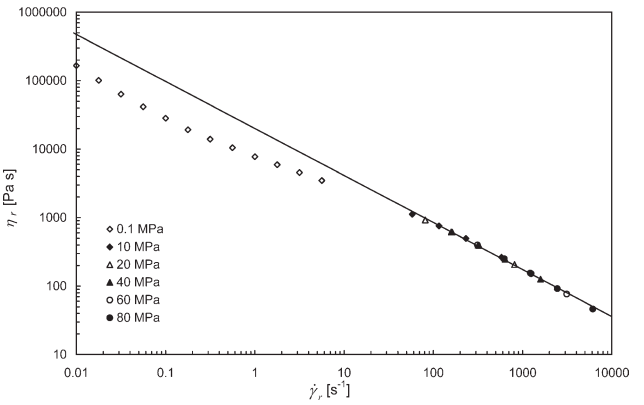

Figure 9 Reduced viscosity (= η/α_p) vs. reduced shear rate (=$\alpha_p\dot{\gamma}$) for ABS with eq. (10); the line represents the prediction of the power-law model, eq. (13) based on the capillary rheometer data. The best-fit parameter values are given in Table I.

calculate β at different temperatures from the model parameters of their study. For comparison in Table II, this relation was used to calculate the values of β at temperatures corresponding to our experiments.

Inspection of Table II reveals that some differences between the present and previous results do exist. For PS, PP, and LDPE, however, all the pressure coefficients are relatively close to each other. For PC and ABS the discrepancy appears to be larger, but for both of these materials there is only one previous value to be used for comparison. It is worth mentioning that for PC slightly lower values of β were reported at both 280 and 300°C (29.4 and 30.4 GPa^{-1}, respectively) than at 290 °C.[18] In the case of ABS, there may be differences in the material composition (in the butadiene content, for example). Namely, unlike in the present study, in the study of Kadijk and van den Brule[7] the ABS polymer used seems to have a zero-shear-rate viscosity (even though it was not strictly reached in the experiments). It is also possible that the determination of β in the present study includes some inaccuracies due to the fitting defect associated with the yield stress behavior of ABS.

Obviously, the complexity of the molecular structure gives a guideline for assessing the degree of pressure dependence: Not surprisingly, the amorphous polymers (PS, ABS, and PC) with a more complex molecular structure have higher pressure coefficients than the semicrystalline polymers (PP and LDPE). Nevertheless, more complex molecular interactions, such as stiffness of the backbone and bulkiness of the pendant groups, also play a role as quoted in the introduction. In addition, also the molecular architecture should be accounted for: In the case of polyethylene the branched—especially long-chain branched—polymer chains possess larger intermolecular free volume than the linear ones,

TABLE II
Comparison of Pressure Coefficients β (GPa^{-1})

	Present study	Kadijk and van den Brule[7]	Couch and Binding[15]	Sedlacek et al.[18]
PC	26.6 (290°C)	–	–	33.6 (290°C)
PS	35.5 (200°C)	37.7 (200°C)	29.0 (200°C)	40.7 (210°C)
PP	20.5 (220°C)	17.7 (220°C)	21.5 (230°C)	20.6 (210°C)
LDPE	17.6 (200°C)	–	16.0 (200°C)	18.3 (190°C)
ABS	33.7 (230°C)	24.5 (230°C)	–	–

being more sensitive to the changes in pressure.[35] On the other hand, the contribution of free volume to the pressure dependence varies among different polymers; for example for polystyrene, it seems to have a greater role, whereas for polyethylene thermal activation is more important.[36]

From the molecular structure it is not self-evident that the pressure coefficient of PS, 35.5 GPa^{-1}, is quite a bit larger than that of PC, 26.6 GPa^{-1}. The explanation for this is probably to be found in the temperature dependence of β. More specifically, the testing temperature of PC, 290°C, is more above the glass transition temperature ($T_g \approx 145$°C[37]; test temperature $T_g + 145$°C) than that of PS ($T_g \approx 95$°C[37]; test temperature $T_g + 105$°C). Thus, it would be interesting to compare the pressure coefficients of PS and PC at corresponding temperatures relative to T_g. Based on the information provided by Kadijk and van den Brule,[7] it is possible to estimate the value of β for PS at 240°C ($\approx T_g + 145$°C); the value obtained doing so, β = 26.8 GPa^{-1}, is indeed nearly identical with the present value of β = 26.6 GPa^{-1} for PC at 290°C.

For the purpose of quantitatively comparing the viscosity values at different pressures, it is useful to rewrite the Carreau-Yasuda equation in the form

$$\eta = \alpha_p \eta_0 \left[1 + (\alpha_p \lambda \dot{\gamma})^a\right]^{(n-1)/a} \tag{14}$$

where α_p is obtained from eq. (10). Let us now consider the viscosity at two different pressures having the pressure shift factors α_{p1} and α_{p2}. It is obvious that the ratio of viscosities at these two pressures (η_2/η_1) varies with shear rate; in the limit of low shear rates η_2/η_1 takes the value of α_{p2}/α_{p1} and at high shear rates it approaches the value of $(\alpha_{p2}/\alpha_{p1})^n$. Taking the parameter values of PS in Table I to calculate α_p at 0.1 and 80 MPa, we obtain the values of 1 and 17.1, respectively. Thus, in the limiting regions of low and high shear rates the viscosity ratios become 17.1 and 2.28, respectively. If we consider the fully developed isothermal flow between infinite parallel plates, which roughly approximates the flow during injection mold filling, we can expect the ratio of pressure gradients needed to drive the flow to be comparable with the ratio of viscosities. That is, with similar flow rates the pressure gradients corresponding to the pressure level of 80 MPa are higher by a factor of 2.28 or more than those corresponding to 0.1 MPa. In reality, the pressures in the injection molding process may be even 200 MPa. Hypothesizing that the pressure shift factor of PS can be represented by eq. (10) with β = 35.5 GPa^{-1} up to 200 MPa, we obtain $\alpha_p = 1208$ at 200 MPa. This means that in the asymptotic limit of high shear rates the viscosity at 200 MPa is higher by a factor of 7.8 than that at 0.1 MPa.

A few comments are worth making with respect to the aforementioned discussion. First, the discussion was based on the data of PS, whose viscosity is highly sensitive to pressure. For LDPE, for example, the pressure effect is much smaller. Second, the nonisothermal effects always play a significant role in the injection molding process and therefore the conclusions based on the isothermal assumption may be more or less misleading. Third, when the viscosity is measured with a standard capillary rheometer, the pressure is atmospheric only at the exit of the capillary and hence the viscosity results invariably include some, albeit arbitrary, pressure effect.

CONCLUSIONS

Viscosity measurements at elevated pressures were conducted on several polymers using a capillary rheometer equipped with a pressurizable downstream chamber. The fitting procedure utilizing the time-pressure superposition principle and the Carreau-Yasuda viscosity model was used to determine the pressure coefficient from the experimental data. The results, which are in reasonable accordance with previous ones, reveal significant pressure dependence of viscosity particularly for amorphous polymers PS, ABS, and PC. When injection molding of polymers is considered, a feature accounting for the pressure dependence of viscosity should obviously be included in the simulations of injection molding in order to get realistic predictions particularly for polymers whose viscosity significantly depends on pressure.

The authors thank Semu Salmivalli and Juha-Pekka Pöyry for assisting in experimental work.

References

1. García, S.; Roldán, A.; Hernández, J. P.; Osswald, T. SPE ANTEC Tech Pap 2004, 50, 3418.
2. Maxwell, B.; Jung, A. Mod Plast 1957, 35, 174.
3. Westover, R. C. Polym Eng Sci 1961, 6, 83.
4. Ito, K.; Tsutsui, M.; Kasajima, M.; Ojima, T. Appl Polym Symp 1973, 20, 109.
5. Karl, V. H. Angew Makromol Chem 1979, 79, 11.
6. Mackley, M. R.; Spitteler, P. H. J. Rheol Acta 1996, 35, 202.
7. Kadijk, S. E.; Van Den Brule, B. H. A. A. Polym Eng Sci 1994, 1535.
8. Duvdevani, I. J.; Klein, I. SPE J 1967, 23, 41.
9. Penwell, R. C.; Porter, R. S. J Polym Sci 1971, 9, 463.
10. Liang, J.-Z. Polymer 2001, 42, 3709.
11. Pantani, R.; Sorrentino, A. Polym Bull 2005, 54, 365.
12. Laun, H. M. Rheol Acta 1983, 22, 171.
13. Driscoll, P. D.; Bogue, D. C. J Appl Polym Sci 1990, 39, 1755.
14. Couch, M. A.; Binding, D. M.; Walters, K. J Non-Newtonian Fluid Mech 1999, 79, 137.
15. Couch, M. A.; Binding, D. M. Polymer 2000, 41, 6323.
16. Goubert, A.; Vermant, J.; Moldenaers, P.; Göttfert, A.; Ernst, B. Appl Rheol 2001, 11, 26.
17. Laun, H. M. Rheol Acta 2003, 42, 295.
18. Sedlacek, T.; Zatloukal, M.; Filip, P.; Boldizar, A.; Sáha, P. Polym Eng Sci 2004, 44, 1328.
19. Carreras, E. S.; Kissi, N. E.; Piau, J. M.; Toussaint, F.; Nigen, S. Rheol Acta 2006, 45, 209.
20. Cardinaels, P.; Van Puyvelde, P.; Moldenaers, P. Rheol Acta 2007, 46, 495.
21. Hellwege, V. K. H.; Knappe, W.; Paul, F.; Semjonov, V. Rheol Acta 1967, 8, 165.
22. Christmann, L.; Knappe, W. Rheol Acta 1976, 15, 296.
23. Cogswell, F. N. Plast Polym 1973, 41, 39.
24. Koran, F.; Dealy, J. M. J Rheol 1999, 43, 1279.
25. Ferry, J. D. Viscoelastic Properties of Polymers; 3rd ed.; Wiley: New York, 1980.
26. Utracki, L. A. Polym Eng Sci 1983, 23, 446.
27. Utracki, L. A.; Sedlacek, T. Rheol Acta 2007, 46, 479.
28. Sedlacek, T.; Cermak, R.; Hausnerova, B.; Zatloukal, M.; Boldizar, A.; Saha, P. Int Polym Process XX 2005, 3, 286.
29. Fernández, M.; Muñoz, M. E.; Santamaría, A. Macromol Chem Phys 2008, 209, 1730.
30. Aho, J.; Syrjälä, S. Appl Rheol 2008, 18, 63258.
31. Chmiel, H.; Schümmer, P. Chem Ing Tech 1971, 43, 1257.
32. Schümmer, P.; Worthoff, R. H. Chem Eng Sci 1978, 33, 759.
33. Hieber, C. A. In Injection and Compression Molding Fundamentals, Isayev, A. I., Ed.; Marcel Dekker: New York, 1987.
34. Münstedt, H. Polym Eng Sci 1981, 21, 259.
35. Sedlacek, T.; Lengalova, A.; Zatloukal, M.; Cermak, R.; Saha, P. Int Polym Process XXI 2006, 2, 98.
36. Park, H. E.; Dealy, J.; Münstedt, H. Rheol Acta 2006, 46, 153.
37. Brydson, J. A. Handbook for Plastics Processors; Heinemann Newnes: Oxford, 1990.